



Universiteit
Leiden

The Netherlands

Refinement of antisense oligonucleotide mediated exon skipping as therapy for Duchenne muscular dystrophy

Heemskerk, J.A.

Citation

Heemskerk, J. A. (2011, October 26). *Refinement of antisense oligonucleotide mediated exon skipping as therapy for Duchenne muscular dystrophy*. Retrieved from <https://hdl.handle.net/1887/17986>

Version: Corrected Publisher's Version

License: [Licence agreement concerning inclusion of doctoral thesis in the Institutional Repository of the University of Leiden](#)

Downloaded from: <https://hdl.handle.net/1887/17986>

Note: To cite this publication please use the final published version (if applicable).

Chapter 4

Pre-clinical PK and PD studies on 2'O-methyl-phosphorothioate RNA antisense oligonucleotides in the *mdx* mouse model

Heemskerk H¹, de Winter CL¹, van Kuik-Romeijn P², Heuvelmans N²,
Sabatelli P^{3,4}, Rimessi P³, Braghetta P⁵, van Ommen GJB¹, de Kimpe S²,
Ferlini A³, van Deutekom JCT² and Aartsma-Rus A¹

¹Human Genetics, Leiden University Medical Center, the Netherlands

²Prosensa Therapeutics, the Netherlands

³Experimental and Diagnostic Medicine, Section of Medical Genetics,
University of Ferrara, Italy

⁴IGM-CNR, Unit of Bologna c/o IOR, Italy

⁵Histology, Microbiology, and Medical Biotechnology, University of
Padova, Italy

Molecular Therapy (2010) 18(6), 1210-7

Preclinical PK and PD Studies on 2'-O-Methyl-phosphorothioate RNA Antisense Oligonucleotides in the *mdx* Mouse Model

Hans Heemskerck¹, Christa de Winter¹, Petra van Kuik², Niki Heuvelmans², Patrizia Sabatelli^{3,4}, Paola Rimessi³, Paola Braghetta⁵, Gert-Jan B van Ommen¹, Sjeff de Kimpe², Alessandra Ferlini³, Annemieke Aartsma-Rus¹ and Judith CT van Deutekom^{1,2}

¹Center for Human and Clinical Genetics, Leiden University Medical Center, Leiden, The Netherlands; ²Prosensa Therapeutics B.V., Leiden, The Netherlands; ³Department of Experimental and Diagnostic Medicine, Section of Medical Genetics, University of Ferrara, Ferrara, Italy; ⁴IGM-CNR, Unit of Bologna c/o IOR, Bologna, Italy; ⁵Department of Histology, Microbiology, and Medical Biotechnology, University of Padova, Padova, Italy

Antisense oligonucleotides (AONs) are being developed as RNA therapeutic molecules for Duchenne muscular dystrophy. For oligonucleotides with the 2'-O-methyl-phosphorothioate (2OMePS) RNA chemistry, proof of concept has been obtained in patient-specific muscle cell cultures, the mouse and dog disease models, and recently by local administration in Duchenne patients. To further explore the pharmacokinetic (PK)/pharmacodynamic (PD) properties of this chemical class of oligonucleotides, we performed a series of preclinical studies in mice. The results demonstrate that the levels of oligonucleotides in dystrophin-deficient muscle fibers are much higher than in healthy fibers, leading to higher exon-skipping levels. Oligonucleotide levels and half-life differed for specific muscle groups, with heart muscle showing the lowest levels but longest half-life (~46 days). Intravenous (i.v.), subcutaneous (s.c.), and intraperitoneal (i.p.) delivery methods were directly compared. For each method, exon-skipping and novel dystrophin expression were observed in all muscles, including arrector pili smooth muscle in skin biopsies. After i.v. administration, the oligonucleotide peak levels in plasma, liver, and kidney were higher than after s.c. or i.p. injections. However, as the bioavailability was similar, and the levels of oligonucleotide, exon-skipping, and dystrophin steadily accumulated overtime after s.c. administration, we selected this patient-convenient delivery method for future clinical study protocols.

Received 29 September 2009; accepted 30 March 2010; published online 20 April 2010. doi:10.1038/mt.2010.72

INTRODUCTION

The severe and progressive deterioration of muscle fibers in Duchenne muscular dystrophy (DMD) is caused by the deficiency of dystrophin, a protein that is essential for the integrity of muscle

fiber membranes.¹ In DMD patients, mutations in the *DMD* gene, mostly deletions of one or more exons (~72%),² disrupt the open reading frame of the transcript and prematurely abort the synthesis of the dystrophin protein.³ Patients with Becker muscular dystrophy show intermediate-to-milder phenotypes with mostly longer-to-normal life expectancies when compared with DMD patients. Here, the mutations in the *DMD* gene maintain the open reading frame and result in an internally truncated but semifunctional dystrophin.^{3,4}

Antisense oligonucleotides (AONs) are innovative synthetic drugs currently being developed for the treatment of DMD.⁵ Based on specific chemical modifications their mechanism of action here is not RNase H-mediated cleavage of target RNA, but instead induction of specific exon-skipping by disturbing exon inclusion signals during pre-mRNA splicing. Mutation-specific targeted skipping of 1 or more exons in DMD patients allows restoration of the mutated open reading frame, introduction of novel dystrophin synthesis, and conversion of a severe DMD into a (much) milder Becker muscular dystrophy phenotype.⁵

Two different AON chemistries are currently being studied extensively toward clinical application: 2'-O-methyl-phosphorothioate (2OMePS) RNA and phosphorodiamidate morpholino oligomer (PMO).⁶ Both have been shown to be effective in inducing exon-skipping and dystrophin restoration in cultured muscle cells from a series of DMD patients with different mutations, in the *mdx* and transgenic human DMD mouse models, and in the DMD dog model.⁷⁻¹⁵ Peptide conjugated PMOs were more efficient than their unconjugated counterpart, especially in heart.^{16,17}

Although PMO targeting mouse exon 23 appears to be more effective than 2OMePS, this difference was not observed for human target exons.⁶ AONs of both chemistries targeting exon 51 were equally efficient in human proof-of-concept studies.¹⁸ The first trial involved PRO051 (2OMePS).¹⁹ Four Dutch DMD patients received an intramuscular (i.m.) injection of a single dose (0.8 mg). The compound was safe, well-tolerated, and effective in specifically inducing exon 51 skipping and dystrophin restoration

Correspondence: Annemieke Aartsma-Rus, Center for Human and Clinical Genetics, Postzone S4-P, Leiden University Medical Center, PO Box 9600, 2300 RC Leiden, The Netherlands. E-mail: a.m.rus@lumc.nl

(up to 35%) in the majority of muscle fibers (up to 97%) in the treated area. Recently, i.m. injection of 0.9 mg AVI-4658 (PMO) in five DMD patients also demonstrated to be well-tolerated, inducing dystrophin levels of up to 32% in 79% of the fibers in the treated area.²⁰

Although both studies confirm proof of concept, they only resulted in local dystrophin synthesis. To allow body-wide production, systemic AON delivery is required. Intravenous (i.v.) delivery of a mouse exon 23-specific 2OMePS AON (23AON) in *mdx* mice previously showed whole-body dystrophin, albeit at variable levels: minimal in heart, high in gastrocnemius muscle.²¹ Interestingly, early signs for effective accumulation were observed; after three injections of the 23AON the levels of dystrophin that accumulated were comparable with levels observed after one injection.

For future clinical studies on systemic delivery of AONs, more extensive pharmacokinetic (PK) and pharmacodynamic (PD) studies are required to determine the optimal dose, regimen, route of administration, and accordingly biodistribution, clearance, muscle specific uptake, and AON half-life. Here, we describe a series of PK/PD experiments in *mdx* mice as part of the preclinical development of 2OMePS AONs for DMD.

RESULTS

Enhanced levels of 2OMePS RNA AONs in dystrophic muscle

PK data on AONs are fundamental for the optimization of dose and regimen for systemic treatment of DMD patients, especially because this treatment will be chronic. Here, we applied a quantitative and sequence-specific hybridization ligation assay to study the biodistribution of 2OMePS RNA AONs upon systemic delivery.⁶ First, we confirmed a previously observed phenomenon of enhanced exon-skipping efficiencies in dystrophic muscle when compared to healthy muscle.¹¹ Both wild-type and *mdx* mice ($n = 3$, similar age) received a single i.v. 50 mg/kg dose of a mouse-specific 2OMePS RNA AON, inducing exon 23 skipping [M23D(+02–18)].^{21,22} At 48 hours postinjection, the gastrocnemius and triceps muscles showed four and eight times higher 23AON levels (up to 10 $\mu\text{g/g}$), respectively, in *mdx* mice than in wild-type mice (Figure 1a). The 23AON levels in heart were markedly lower but still 2.5 times higher in *mdx* than in wild-type mice. This differential uptake was not observed in kidney and liver, which showed high (up to 100 $\mu\text{g/g}$) but equal levels of 23AON in both mouse groups. These results confirm that there is an enhanced absorption of 23AON from the blood circulation, probably due to the myogenic degeneration and regeneration processes in the *mdx* mice, associated with a higher permeability of the myofiber membranes and/or vascular system.

In a related experiment, the levels of exon 23 skipping in wild-type versus *mdx* mice ($n = 3$, similar age) were monitored over a period of 2 weeks after two 20- μg i.m. injections (24-hour interval) of the 23AON (Figure 1b). In wild-type mice, the levels were very low, up to 2% at 4 days after treatment. Given the lower 23AON levels in healthy muscle, this was anticipated. In contrast, in the *mdx* mice exon 23 skipping levels were 4–20 times higher than in wild-type mice, and increased over time up to 20% at 10 days postinjection. This PD pattern suggests that 2OMePS RNA AONs

are stable within muscle fibers, and that the levels of in-frame transcript after exon 23 skipping can therefore accumulate over time.

Half-life of 2OMePS RNA AONs in *mdx* tissue

To study the stability (half-life) of 2OMePS RNA AONs in *mdx* muscle tissue, a series of *mdx* mice were given three i.v. injections of 100 mg/kg 23AON in 1 week (every other day). At 2, 4, 7, and 14 days after the last injection, two mice were killed for analysis. AON levels were assessed in the gastrocnemius, triceps, and quadriceps muscles, heart, kidney, and liver (Figure 2a). The uptake of the compound by the kidney and liver was higher (up to 10 times) than in skeletal muscle. However, the relative clearance was also markedly faster. The levels of AON in the different skeletal muscle groups were similar (36–45 $\mu\text{g/g}$) at day 2 and persisted for at least 14 days at levels of ~40% (gastrocnemius and quadriceps) and 78% (triceps). The lowest levels of AON were observed in the heart (11 $\mu\text{g/g}$), but 80% of this was still detected after 14 days. Based on these data, the half-life of the 2OMePS 23AON was determined for different tissues (Figure 2b) and was found to be similar in the gastrocnemius and quadriceps muscles (~10 days), but markedly higher in the triceps muscle (~33 days). This may have been due to a lower extent of degeneration and regeneration in the higher extremities, and/or to a differential type I/II fiber content. The same phenomenon may explain the markedly longer half-life of the AON in cardiac muscle tissue (~46 days). This observation is encouraging because it implies that the relatively low 2OMePS RNA AON levels in heart may be compensated overtime by a prolonged persistence and thus accumulation of AON in repeated-dosing studies.

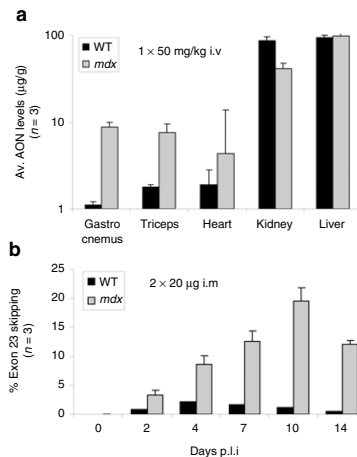


Figure 1 Enhanced levels of 2OMePS RNA AONs in dystrophic muscle. **(a)** Comparison of AON levels in skeletal muscles (gastrocnemius and triceps muscle), heart, kidney, and liver from wild-type (WT) versus *mdx* mice ($n = 3$), after a single intravenous (i.v.) injection of 50 mg/kg mouse exon 23-specific 2'-O-methyl-phosphorothioate antisense oligonucleotide (23AON). **(b)** Comparison of exon 23 skipping levels in gastrocnemius muscles from series of WT versus *mdx* mice ($n = 3$), at different time points (up to 14 days) after 2 intramuscular (i.m.) injections of 20 μg 23AON (with 24-hour interval).

The effect of different routes of administration on 20MePS RNA AON pharmacokinetics

The route of administration affects the PK characteristics of therapeutic molecules. We therefore evaluated the PK/PD profiles of the 23AON after i.v., intraperitoneal (i.p.), subcutaneous (s.c.), and i.m. injections in *mdx* mice (all at age ~3 weeks) from different

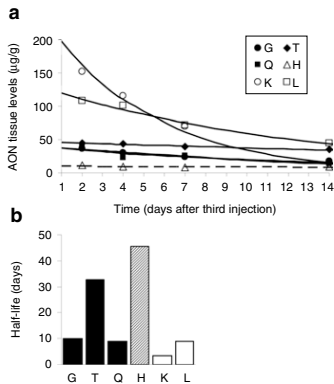


Figure 2 Half-life of 20MePS RNA AONs in *mdx* tissue. **(a)** Antisense oligonucleotide (AON) tissue levels in gastrocnemius (G), triceps (T), quadriceps (Q), heart (H), kidney (K), and liver (L) of *mdx* mice after three intravenous injections of 100 mg/kg mouse exon 23–specific 2'-*O*-methyl-phosphorothioate AON (23AON), monitored from 2 to 14 days postinjection. **(b)** The half-life of the 23AON in different muscle groups and organs.

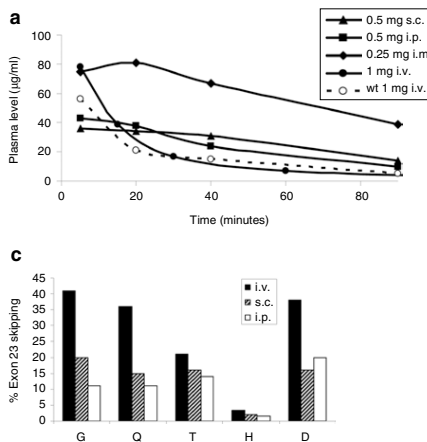


Figure 3 The effect of different routes administration on 20MePS RNA AON pharmacokinetics. **(a)** Antisense oligonucleotide (AON) plasma levels in *mdx* mice after single intramuscular [i.m., 0.25 mg (12.5 mg/kg)], intravenous [i.v., 1 mg (50 mg/kg)], intraperitoneal [i.p., 0.5 mg (25 mg/kg)], or subcutaneous [s.c., 0.5 mg (25 mg/kg)] injections of mouse exon 23–specific 2'-*O*-methyl-phosphorothioate AON (23AON), monitored from 5 to 90 minutes after injection, and compared with those after a single i.v. injection of 1 mg (50 mg/kg) in wild-type (WT) mice. **(b)** AON tissue levels in pooled skeletal muscle samples of treated *mdx* mice compared with those in kidney (K) and liver (L) after five i.v., s.c., or i.p. injections of 250 mg/kg in 1 week. **(c)** The corresponding exon 23 skipping levels in gastrocnemius (G), quadriceps (Q), triceps (T), heart (H), and diaphragm (D) after i.v., s.c., or i.p. injections. **(d)** Western blot analysis of total protein extracts isolated from Q, T, and H muscle of three *mdx* mice, all treated with five 250 mg/kg i.v. injections of 23AON, compared with a healthy muscle sample [healthy control (HC); diluted 1/25 to avoid overexposure].

independent experiments. First, the effect of the different routes of administration on AON plasma levels and clearance was assessed (Figure 3a). After a single i.v. injection of 50 mg/kg (~1 mg/animal) 23AON, the levels in plasma 5 minutes postinjection were high (78 µg/ml), with almost complete clearance after 90 minutes. This pattern was similar in wild-type mice. I.p. and s.c. injections of half this dose (25 mg/kg) in *mdx* mice resulted in twofold lower plasma levels (43 and 36 µg/ml, respectively), and a slower clearance than i.v. injection. Remarkably, we observed relatively high and sustained AON plasma levels (50–60 µg/ml) after a single i.m. injection of 12.5 mg/kg (0.25 mg/animal) of 23AON. These results suggest that there is a delayed and continuing release of AON from bodily tissue to the blood circulation, which is especially significant in *mdx* muscle tissue (still at 39 µg/ml after 90 minutes).

To further study the extent of the whole-body therapeutic effects after AON treatment and to enhance any potential PK/PD differences between the delivery methods studied, we then compared the different routes of administration at a high dose of 250 mg/kg 23AON. Sets of three *mdx* mice received 250 mg/kg of 23AON five times in 1 week by either i.v., i.p., or s.c. injections. They were killed at 3 days after the last injection. The relative levels of AON in different muscle groups, being on average 5–10 times lower than in kidney and liver, did vary slightly with the different routes of administration: ~1.3 times higher levels after i.v. versus i.p. or s.c. administration (Figure 3b). The effect of delivery method on the kidney and the liver levels was much stronger. I.v. injections resulted in the highest acute levels of AON in kidney (725 µg/g) and liver (650 µg/g) when compared with the i.p. (345 and 235 µg/g, respectively) and s.c. (355 and 275 µg/g, respectively) injections. Therefore, at this dose

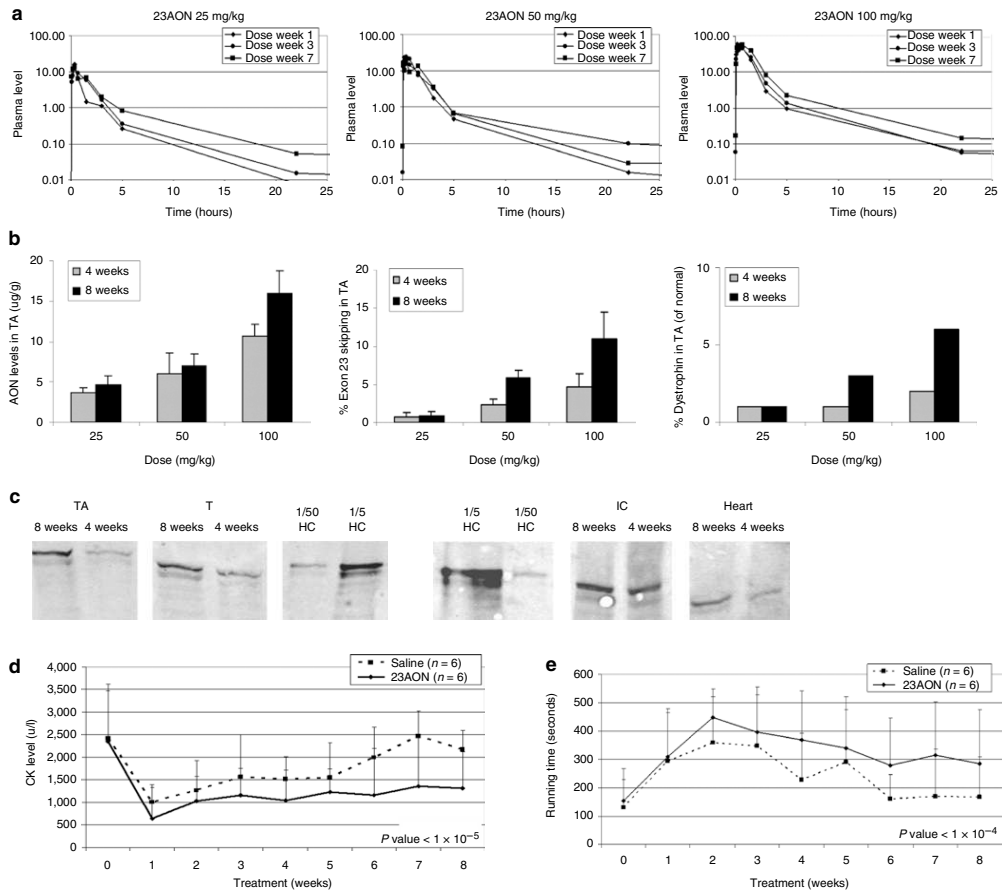


Figure 4 Optimization of PK and PD profiles of 2OMEps RNA AONs in *mdx* mice after s.c. administration. **(a)** Antisense oligonucleotide (AON) plasma levels in *mdx* mice after 25, 50, or 100 mg/kg subcutaneous (s.c.) injections (2/week) for up to 8 weeks, monitored from 0.5 to 22 hours after dosing at week 1, 3, and 7. **(b)** AON tissue levels, exon 23 skipping levels, and dystrophin levels in tibialis anterior (TA) muscles from *mdx* mice treated with 25, 50, or 100 mg/kg s.c. injections (2/week) for 4 or 8 weeks. **(c)** Western blot analysis of total protein extracts isolated from tibialis anterior (TA), triceps (T), intercostal (IC), and heart (H) muscle of *mdx* mice after 100 mg/kg s.c. injections (2/week) for 4 or 8 weeks. Wild-type muscle (HC) was used as a positive control and diluted 5 and 50 times (1/5 and 1/50, respectively). The three panels on the left are from one blot, the three panels on the right from another (spaces indicate the removal of irrelevant samples). **(d)** Average plasma creatine kinase (CK) levels in treated [100 mg/kg mouse exon 23–specific 2'-*O*-methyl-phosphorothioate AON (23AON), s.c.] and untreated (saline, s.c.) *mdx* mice over time up to 8 weeks. The difference between treated and untreated is significant (P value = 6.36×10^{-6}). **(e)** Corresponding Rotarod running time (seconds) of treated versus untreated mice over time up to 8 weeks. The difference is significant (P value = 1.77×10^{-5}).

and regimen, i.v. injections may be less tolerable. I.p. and s.c. injections clearly showed a less acute PK pattern in kidney and liver.

The typical PK profile as per route of administration directly correlated with the PD effects in muscle. The levels of exon 23 skipping in a series of skeletal muscle groups, the heart, and diaphragm, isolated from the same set of treated *mdx* mice demonstrated that the i.v. route of administration did allow the highest levels of exon-skipping (up to 43% of total transcripts in

the quadriceps and 4% in heart; **Figure 3c**). With the i.p. and s.c. routes the percentages of exon 23 skipping were typically lower: 40–80% (s.c.) and 30–70% (i.p.) of those obtained after i.v. administration, depending on the specific muscle group analyzed. Independent of the administration route, the exon 23 skipping levels varied between the specific muscle groups analyzed, with the highest levels in the quadriceps and gastrocnemius muscles. This correlates with the higher AON levels in these muscles when compared, for instance, to the triceps muscle (**Figure 2a**).

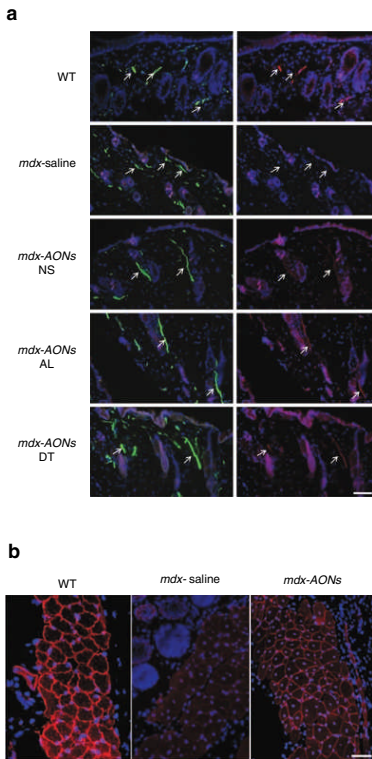


Figure 5 Dystrophin restoration in skin arrector pili. **(a)** Dystrophin and desmin immunofluorescence staining of arrector pili smooth muscle in skin biopsies from neck scruff (NS), anterior leg (AL) and dorsal tail regions (DT) from treated (s.c., 100 mg/kg) and untreated (saline) *mdx* mice versus wild-type mice. Desmin (green) colocalizes with dystrophin (red) and is expressed in all animals. No dystrophin labeling was detected in untreated animals, while dystrophin is expressed in all treated and wild-type animals. Bar = 400 μ m. **(b)** Dystrophin immunofluorescence staining of panniculus carnosus in skin biopsy from the DT in wild-type (left panel), untreated (middle panel), and treated (right panel) mice. Dystrophin labeling is intense and continuous at the sarcolemma of muscle fibers of panniculus carnosus of wild-type skin biopsy and absent in *mdx* mice. In *mdx* mice treated with AONs, dystrophin labeling is detected at the sarcolemma of muscle fibers with an almost continuous pattern. All samples were photographed at the same exposition time and the images were not differently manipulated. Nuclei are stained with DAPI. Bar = 200 μ m.

Differences in muscle group-specific response to 23AON were also observed on protein levels. Western blot analysis of total protein extracts from the quadriceps, triceps, and heart muscles of the mice that were treated by i.v. injection demonstrated generally higher dystrophin levels in the quadriceps than the triceps muscles (Figure 3d). Relatively high levels of dystrophin expression were observed in the heart samples. This may at least partly be explained by the longer half-life of the 23AON in the heart (Figure 2b).

Optimization of PK and PD profiles of 20MePS RNA AONs in *mdx* mice after s.c. administration

Given the lower acute 23AON plasma levels and lower liver and kidney load after s.c. administration, we further focused on s.c. dosing and regimen. Groups of *mdx* mice received s.c. doses of 25, 50, or 100 mg/kg of 23AON twice weekly, over a period of 4 or 8 weeks. Saline-treated mice were used as a control group. No behavioral differences were observed between AON-treated and saline-treated mice throughout the treatment period. Following these treatments, different serum parameters (glutamic-oxaloacetic transaminase, ureas, hemoglobin, creatine, alkaline phosphatase, and glutamic-pyruvic transaminase) were assessed and did not indicate toxic effects on liver and kidney (data not shown). In addition, the weight of liver, kidney, and spleen did not differ between treated and nontreated animals.

AON pharmacokinetics and overall muscle integrity and function were assessed during and after treatment. First, for each dose, 23AON plasma levels were assessed over time (Figure 4a). Increasing doses resulted in increasing plasma peak levels, but per dose, these peak levels did not increase over time; similar levels were obtained in either weeks 1, 3, and 7. The 23AON was rapidly cleared from the blood circulation, which may reflect a fast and significant absorption by the dystrophic muscle tissue. In contrast to the plasma peak levels, the plasma trough levels showed a steady accumulation over time and at increased levels (i.e., total plasma exposure) with increased dose. These levels most likely correlated to the muscle tissue exposure and to the PD response therein. In fact, the levels of 23AON in the tibialis anterior muscle demonstrated accumulation of the compound over time, and increased per subsequent higher dose group (Figure 4b, left panel). These dose-dependent PK profiles directly correlated with the levels of exon 23 skipping and dystrophin expression in the same tibialis anterior muscle (Figure 4b, middle and right panels). Tissue levels of $\sim 4 \mu\text{g/g}$ were sufficient to induce low levels of exon-skipping. By contrast, for the highest dose (100 mg/kg), the exon 23 skipping level was up to 11% after 8 weeks, with associated dystrophin levels up to 6% of that in normal muscle tissue (Figure 4c).

Plasma creatine kinase (CK) levels were also determined weekly during treatment (Figure 4d). CK is a muscle enzyme that leaks into the bloodstream when muscle fibers are damaged and is therefore considered an early biomarker for muscle integrity. In untreated *mdx* mice, the CK levels vary but are typically elevated to 1,500–3,000 U/l. For the *mdx* mice in the 100 mg/kg group, the CK levels were found to be significantly lower over time (P value $< 1 \times 10^{-5}$) than those in the saline-treated mice, whereas they were comparable before treatment. The seemingly increased muscle fiber integrity in the mice in this high-dose group probably contributed to the improved muscle performance as observed by Rotarod analysis over time (Figure 4e). Both the saline and the 100 mg/kg 23AON-treated mice showed increased running times during the first 2 weeks (learning curve), but then running times decreased after 2 weeks. However, the decline for the 23AON-treated mice was much more gradual than for saline-treated mice. In addition, the plateau level of treated mice was higher (300 seconds versus ~ 170 seconds). This difference between the untreated and treated groups was significant over time (P value $< 1 \times 10^{-4}$).

Dystrophin restoration in skin arrector pili

For six mice treated with 100 mg/kg 23AON s.c., dystrophin restoration was monitored in smooth muscle of the skin (arrector pili muscle). It was previously demonstrated that skin biopsies may be used for the diagnosis of DMD or Becker muscular dystrophy on the basis of immunostaining of dystrophin in arrector pili muscles.^{23,24} In addition, we recently demonstrated dystrophin restoration after treatment of 2OMePS AONs complexed with nanoparticles in the *mdx* mouse model.²⁵ Indeed, in the three mice receiving 8 weeks of 23AON treatment, clear dystrophin signals were observed in the arrector pili muscles all over the skin (anterior leg, dorsal tail region, neck scuff region; **Figure 5a**). Dystrophin restoration was also clearly visible in the panniculus carnosus, a skeletal muscle layer of the skin (**Figure 5b**). The immunostaining patterns obtained were similar to those observed in healthy wild-type mice, whereas no dystrophin signals were observed in the saline-treated mice.

DISCUSSION

Two different AON chemistries are most advanced in preclinical and clinical development for DMD: 2OMePS RNA and PMO. Although their modes of action are identical, 2OMePS and PMO compounds have significantly different chemical structures and associated characteristics and, even when targeting an identical sequence, require independent toxicity and PK versus PD studies. Before clinical studies applying systemic delivery of 2OMePS compounds, we performed a large series of preclinical PK/PD studies in the *mdx* mouse model with a mouse exon 23–specific compound of the same chemistry. The effects of dose, regimen, treatment period, and route of administration on biodistribution, specific muscle tissue availability, and molecular response were assessed.

For the biodistribution studies a quantitative and AON sequence-specific hybridization ligation assay was applied. It allowed quantification of AON levels in plasma but also in different tissues and organs, albeit without discrimination between internalized and still-circulating molecules.⁶ One of our first observations was that, in *mdx* mouse muscle, higher levels of 23AON were present than in healthy mouse muscle. As this was correlated with similarly higher levels of exon-skipping, these results confirm the increased membrane permeability of dystrophin-deficient and regenerating muscle fibers.²⁶ Therefore, in contrast to many other disease applications, 2OMePS AONs for DMD do not need targeting or uptake-enhancing moieties or formulations to reach sufficient therapeutic levels. This also indicates that studies on 2OMePS AONs in healthy animals or human volunteers are of limited use because the AON absorption by healthy muscle fibers is low and the biodistribution and related possible toxicity profiles are quite different from that in DMD patients. It has been postulated that AONs diffuse into the muscle fibers through the same “holes” from which CK leaks out.²⁶ As elevated CK levels are present in Becker patients as well, it is anticipated that the enhanced absorption of AONs will continue even upon restoration of the Becker-like dystrophin. This would also explain why exon-skipping levels in heart were lower. Although dystrophin-negative heart muscle is affected, it does not have the “holes” that help improved AON absorption in skeletal muscle fibers.

Other important PK observations were that not only the levels of AONs but also the half-life of 23AON varied between specific *mdx* muscle groups. Both parameters determine the final molecular response for different muscle groups. In the heart for instance, the initial levels were 3–5 times lower than in skeletal muscle, but based on the 3–5 times longer half-life the dystrophin levels may eventually be similar to those in skeletal muscle. A differential muscle group response, likely caused by specific muscle group function, muscle structure, and/or fiber type content, should be taken into account when designing systemic clinical trials in which specific muscle groups are studied for clinical outcome measures and molecular effect levels. It remains to be determined whether such differences may become more prominent or level out in DMD patients after long-term treatment.

For DMD patients requiring chronic administration of AONs, an s.c. route of administration is clearly preferred. Our studies in *mdx* mice show that the AON bioavailability for muscle tissue is quite similar after i.v. or s.c. delivery. Whereas the levels of exon-skipping were typically higher in most muscle groups after i.v. administration, this was also accompanied by equally higher peak levels of AON in plasma, kidney, and liver. Therefore, the s.c. route was preferred to limit the risk of organ toxicity. In a follow-up study, we thus further studied dose and treatment duration with s.c. injections. Groups of *mdx* mice received increasing doses (25, 50, and 100 mg/kg, twice weekly) and either for 4 or 8 weeks. We clearly observed increasing levels of AON in muscle with increasing doses and also accumulation of AON over time, which was directly correlated with exon-skipping, dystrophin levels, and improved muscle fiber integrity and function. After 8 weeks of treatment, even at the highest dose, steady-state levels were not yet reached. Further studies in *mdx* mice are necessary to determine when steady-state levels are reached using different doses, and what levels of dystrophin (compared to healthy control) are then achieved in the different muscle groups. Based on the observation that both compound and dystrophin levels accumulate over time, multiple low doses may be preferred over fewer high doses to minimize the risk of toxic effects. A similar hypothesis was recently described for PMO in *mdx* mice.²⁷

Finally, we show here that skin biopsies can be used to detect dystrophin restoration in arrector pili smooth muscle after AON treatment. This is an important finding that may have high value in future clinical studies. It is a markedly less invasive method than muscle biopsy sampling (relevant for discussions with medical ethics committees) and may even allow multiple biopsies over time or at different locations to monitor treatment effects.

In conclusion, results from these PK/PD studies on 2OMePS in the *mdx* mouse model have allowed the generation of various PK simulation models and facilitated rational design of toxicity studies as well as a phase I/IIa study on PRO051. We show that 2OMePS AONs are taken up at high levels by dystrophic muscle, that 2OMePS AONs are stable and have a favorable PK profile and that they can easily be delivered by s.c. injections.

MATERIALS AND METHODS

Administration of 2OMePS AONs in *mdx* mice. *Mdx* (C57Bl/10ScSn-*mdx*/J) and wild-type (C57Bl/6) mice were obtained from Charles River Laboratories (Maastricht, the Netherlands). All experiments were authorized

PK/PD AON Studies in mdx Mice

by the animal experimental commission of the Leiden University Medical Center (project no. 00095, 03027, 06061, and 07151). The AON applied in these experiments was a mouse-specific 2OMePS RNA (a full-length phosphorothioate backbone and 2'-O-methyl modified ribose molecules) inducing exon 23 skipping [M23D(+02–18)].²¹ The AON was administered in saline at doses of 12.5, 25, 50, 100, or 250 mg/kg by either i.m., i.v., i.p., or s.c. injections (see **Supplementary Table S1**). For the i.m. injections, mice were anesthetized by i.p. injection of a 1:1 (vol/vol) Hypnorm/Dormicum solution (Janssen Pharmaceutica, Geel, Belgium/Roche Diagnostics, Almere, the Netherlands). In all experiments, groups of at least three mice were used, typically around 3–4 weeks of age. For plasma PK analysis, a series of blood samples were collected directly after dosing, from 0.5 to 90 minutes. Mice were killed at different time points after the last injection (2–14 days). Different skeletal muscle groups, heart, kidney, and liver were isolated and frozen in liquid nitrogen-cooled 2-methylbutane.

AON hybridization ligation assay. The assay for measuring the concentration of 2OMePS oligoribonucleotide 23AON in plasma and tissue samples is based on a hybridization ligation assay as published by Yu *et al.*²⁸ A template probe (5'-gaatagacagagtaaacggaggtttgcc-biotin-3', 29-mer DNA phosphate oligonucleotide) and a ligation probe (5'-P-cgtctatc-DIG-3', 9-mer DNA phosphate oligonucleotide) were used. The sample was incubated with the template probe (50 nmol/l) at 37°C for 1 hour, and the hybridized samples were transferred to streptavidin-coated 96-well plates. Subsequently, the digoxigenin-labeled ligation probe (2 nmol/l) was added. Detection was performed with anti-DIG-POD (1:4,000; Roche Diagnostics), 3,3',5,5'-tetramethylbenzidine substrate (Sigma Aldrich, Zwijndrecht, the Netherlands), and stop solution (Sigma Aldrich). Absorption at 450 nm was measured in a BioTek Synergy HT plate reader (Beun de Ronde, Abcoude, the Netherlands). The plasma samples were first diluted tenfold with phosphate-buffered saline (PBS) (Invitrogen, Breda, the Netherlands) and subsequent dilutions were done in 1% control mouse plasma (Innovative Research, NIBIO, Amsterdam, the Netherlands) in PBS. The absorption was read against a calibration curve of 23AON prepared in 10% control mouse plasma in PBS. The tissue samples were homogenized to a concentration of 60 mg/ml in proTK buffer (100 mmol/l Tris-HCl, pH 8.5, 200 mmol/l NaCl, 5 mmol/l EDTA, 0.2% sodium dodecyl sulfate) containing 2 mg/ml of proteinase K (Invitrogen), followed by incubation for 2 hours (liver) or 4 hours (kidney, heart, and skeletal muscle) rotating at 55°C in a hybridization oven. Next, the samples were centrifuged for 15 minutes at maximum speed and the supernatant was used in the assay. For liver and kidney samples, all dilutions (at least 200-fold) were done in PBS and the absorption was read against a calibration curve in control liver or kidney diluted in PBS. Heart and muscle samples were first diluted 60-fold in PBS, subsequent dilutions and the calibration curves were done in 60-fold control heart or muscle in PBS.

Reverse transcription-PCR analysis. Muscle samples were homogenized in the RNA-Bee solution (Campro Scientific, Veenendaal, the Netherlands) using a MagNaLyser (Roche Diagnostics) and MagNaLyser green beads (Roche Diagnostics). Total RNA was isolated and purified according to the manufacturer's instructions. For complementary DNA synthesis with Transcriptor Reverse Transcriptase polymerase (Roche Diagnostics), 400 ng of RNA was used in a 20 µl reaction at 60°C for 30 minutes and reverse primed with an exon 25 mouse-specific primer. First, PCRs were performed with outer primers in exons 21 and 26, for 20 cycles of 94°C (40 seconds), 60°C (40 seconds), and 72°C (60 seconds). One microliter of this reaction mixture (diluted 1:10) was then re-amplified using nested primers in exons 22 and 24 with 32 cycles of 94°C (40 seconds), 60°C (40 seconds), and 72°C (60 seconds). PCR products were analyzed on 2% agarose gels. Skipping efficiencies were semiquantitatively determined as percentages of the total (skip and unskipped) amount by quantification of PCR products using the DNA 1000 LabChip Kit and the Agilent 2100 bioanalyzer (Agilent Technologies, Amstelveen, the Netherlands).

Western blot analysis. Western blotting was performed as described.²⁹ Briefly, muscles were homogenized to a concentration of 25 mg/ml in treatment buffer (75 mmol/l Tris-HCl pH 6.8, 15% sodium dodecyl sulfate, 5% β-mercaptoethanol, 2% glycerol, 0.001% bromophenol blue) using MagNa Lyser green beads in the MagNa Lyser. Samples (all ~60 µg protein) were boiled for 5 minutes, loaded on a 4–7% gradient polyacrylamide gel and run overnight at 4°C. Gels were blotted to nitrocellulose BA83 (Whatman, Hertogenbosch, the Netherlands) for 6 hours at 4°C. Blots were blocked with 5% nonfat dried milk (Campina, Rotterdam, the Netherlands) in PBS followed by an overnight incubation with NCL-DYS1 (dilution 1:125; NovaCastra, Newcastle, UK) in Tris-buffered saline plus 0.05% Tween-20 to detect dystrophin. The fluorescent IRDye 800CW goat anti-mouse immunoglobulin (dilution 1:5,000; Li-Cor, Lincoln, NE) was used as a secondary antibody. Blots were visualized and quantified with the Odyssey system and software (Li-Cor).

Immunofluorescence analysis arrector pili muscle. Sections of skin biopsies taken from anterior leg, dorsal tail region, and neck scuff region of treated mdx, untreated mdx, and wild-type mice were labeled with anti-dystrophin antibody (rabbit polyclonal; Santa Cruz Biotechnology, Milan, Italy) and incubated with a TRITC-conjugated secondary antibody (DAKO, Milan, Italy). All samples were double-labeled with an anti-desmin antibody (goat polyclonal 1:10; Santa Cruz Biotechnology) and incubated with anti-goat fluorescein isothiocyanate-conjugated antibody (1:100; Sigma Aldrich). All samples were observed with a Nikon Eclipse 80i fluorescence microscope (Nikon Instruments, Florence, Italy).

CK analysis. Blood was collected in a minicollect tube (Greiner bio-one, Alphen aan de Rijn, the Netherlands) through a small cut at the end of the tail. Serum CK levels were determined using Reflotron CK strips (Roche Diagnostics) in the Reflotron Plus (Roche Diagnostics).

Rotarod analysis. Mice were placed on the Rotarod (Ugo Basile, Comerio, Italy), which accelerated from 5 to 45 r.p.m. in the first 15 seconds. The time spent on the rod was recorded. The session was ended when mice were able to run for 500 seconds. Mice that fell off within 500 seconds were given a maximum of two more tries. The longest running time was used for analyses.

Statistical analysis. Linear regression analyses were performed with the R package (<http://www.Rpackage.org>).

SUPPLEMENTARY MATERIAL

Table S1. Outline of the different experiments.

ACKNOWLEDGMENTS

We are grateful to Maaik van Putten for her help with the statistical analysis. This work was supported by Prosenza Therapeutics and by grants from the Duchenne Parent Project (the Netherlands) and ZonMw (the Netherlands), the TREAT-NMD network of excellence (of which the LUMC and the University of Ferrara are partners), and Telethon (Italy).

REFERENCES

- Hoffman, EP, Brown, RH Jr and Kunkel, LM (1987). Dystrophin: the protein product of the Duchenne muscular dystrophy locus. *Cell* **51**: 919–928.
- Aartsma-Rus, A, Van Deutekom, JC, Folkema, IF, Van Ommen, GJ and Den Dunnen, JT (2006). Entries in the Leiden Duchenne muscular dystrophy mutation database: an overview of mutation types and paradoxical cases that confirm the reading-frame rule. *Muscle Nerve* **34**: 135–144.
- Monaco, AP, Bertelson, CJ, Liechti-Gallati, S, Moser, H and Kunkel, LM (1988). An explanation for the phenotypic differences between patients bearing partial deletions of the DMD locus. *Genomics* **2**: 90–95.
- Hoffman, EP, Fischbeck, KH, Brown, RH, Johnson, M, Medori, R, Loike, JD *et al.* (1988). Characterization of dystrophin in muscle-biopsy specimens from patients with Duchenne's or Becker's muscular dystrophy. *N Engl J Med* **318**: 1363–1368.
- van Ommen, GJ, van Deutekom, J and Aartsma-Rus, A (2008). The therapeutic potential of antisense-mediated exon skipping. *Curr Opin Mol Ther* **10**: 140–149.

6. Heemskerck, HA, de Winter, CL, de Kimpe, SJ, van Kuik-Romeijn, P, Heuvelmans, N, Platenburg, GJ *et al.* (2009). *In vivo* comparison of 2'-O-methyl phosphorothioate and morpholino antisense oligonucleotides for Duchenne muscular dystrophy exon skipping. *J Gene Med* **11**: 257–266.
7. Aartsma-Rus, A, Kaman, WE, Bremmer-Bout, M, Janson, AA, den Dunnen, JT, van Ommen, GJ *et al.* (2004). Comparative analysis of antisense oligonucleotide analogs for targeted DMD exon 46 skipping in muscle cells. *Gene Ther* **11**: 1391–1398.
8. Aartsma-Rus, A, Janson, AA, Kaman, WE, Bremmer-Bout, M, van Ommen, GJ, den Dunnen, JT *et al.* (2004). Antisense-induced multiexon skipping for Duchenne muscular dystrophy makes more sense. *Am J Hum Genet* **74**: 83–92.
9. Alter, J, Lou, F, Rabinowitz, A, Yin, H, Rosenfeld, J, Wilton, SD *et al.* (2006). Systemic delivery of morpholino oligonucleotide restores dystrophin expression bodywide and improves dystrophic pathology. *Nat Med* **12**: 175–177.
10. Arechavala-Gomez, V, Graham, IR, Popplewell, LJ, Adams, AM, Aartsma-Rus, A, Kinali, M *et al.* (2007). Comparative analysis of antisense oligonucleotide sequences for targeted skipping of exon 51 during dystrophin pre-mRNA splicing in human muscle. *Hum Gene Ther* **18**: 798–810.
11. Bremmer-Bout, M, Aartsma-Rus, A, de Meijer, EJ, Kaman, WE, Janson, AA, Vossen, RH *et al.* (2004). Targeted exon skipping in transgenic hDMD mice: a model for direct preclinical screening of human-specific antisense oligonucleotides. *Mol Ther* **10**: 232–240.
12. Lu, QL, Mann, CJ, Lou, F, Bou-Gharios, G, Morris, CE, Xue, SA *et al.* (2003). Functional amounts of dystrophin produced by skipping the mutated exon in the *mdx* dystrophic mouse. *Nat Med* **9**: 1009–1014.
13. Mann, CJ, Honeyman, K, Cheng, AJ, Ly, T, Lloyd, F, Fletcher, S *et al.* (2001). Antisense-induced exon skipping and synthesis of dystrophin in the *mdx* mouse. *Proc Natl Acad Sci USA* **98**: 42–47.
14. McClorey, G, Moulton, HM, Iversen, PL, Fletcher, S and Wilton, SD (2006). Antisense oligonucleotide-induced exon skipping restores dystrophin expression *in vitro* in a canine model of DMD. *Gene Ther* **13**: 1373–1381.
15. Yokota, T, Lu, QL, Partridge, T, Kobayashi, M, Nakamura, A, Takeda, S *et al.* (2009). Efficacy of systemic morpholino exon-skipping in Duchenne dystrophy dogs. *Ann Neurol* **65**: 667–676.
16. Wu, B, Moulton, HM, Iversen, PL, Jiang, J, Li, J, Li, J *et al.* (2008). Effective rescue of dystrophin improves cardiac function in dystrophin-deficient mice by a modified morpholino oligomer. *Proc Natl Acad Sci USA* **105**: 14814–14819.
17. Yin, H, Lu, Q and Wood, M (2008). Effective exon skipping and restoration of dystrophin expression by peptide nucleic acid antisense oligonucleotides in *mdx* mice. *Mol Ther* **16**: 38–45.
18. Aartsma-Rus, A and van Ommen, GJ (2009). Less is more: therapeutic exon skipping for Duchenne muscular dystrophy. *Lancet Neurol* **8**: 873–875.
19. van Deutekom, JC, Janson, AA, Ginjaar, IB, Frankhuizen, WS, Aartsma-Rus, A, Bremmer-Bout, M *et al.* (2007). Local dystrophin restoration with antisense oligonucleotide PRO051. *N Engl J Med* **357**: 2677–2686.
20. Kinali, M, Arechavala-Gomez, V, Feng, L, Cirak, S, Hunt, D, Adkin, C *et al.* (2009). Local restoration of dystrophin expression with the morpholino oligomer AVI-4658 in Duchenne muscular dystrophy: a single-blind, placebo-controlled, dose-escalation, proof-of-concept study. *Lancet Neurol* **8**: 918–928.
21. Lu, QL, Rabinowitz, A, Chen, YC, Yokota, T, Yin, H, Alter, J *et al.* (2005). Systemic delivery of antisense oligonucleotide restores dystrophin expression in body-wide skeletal muscles. *Proc Natl Acad Sci USA* **102**: 198–203.
22. Mann, CJ, Honeyman, K, McClorey, G, Fletcher, S and Wilton, SD (2002). Improved antisense oligonucleotide induced exon skipping in the *mdx* mouse model of muscular dystrophy. *J Gene Med* **4**: 644–654.
23. Marbini, A, Gemignani, F, Bellanova, MF, Guidetti, D and Ferrari, A (1996). Immunohistochemical localization of utrophin and other cytoskeletal proteins in skin smooth muscle in neuromuscular diseases. *J Neurol Sci* **143**: 156–160.
24. Tanveer, N, Sharma, MC, Sarkar, C, Gulati, S, Kaita, V, Singh, S *et al.* (2009). Diagnostic utility of skin biopsy in dystrophinopathies. *Clin Neurol Neurosurg* **111**: 496–502.
25. Ferlini, A, Sabatelli, P, Fabris, M, Bassi, E, Falzarano, S, Vattermi, G *et al.* (2010). Dystrophin restoration in skeletal, heart and skin arrector pili smooth muscle of *mdx* mice by ZM2 NP-AON complexes. *Gene Ther* **17**: 432–438.
26. Hoffman, EP (2007). Skipping toward personalized molecular medicine. *N Engl J Med* **357**: 2719–2722.
27. Malerba, A, Thorogood, FC, Dickson, G and Graham, IR (2009). Dosing regimen has a significant impact on the efficiency of morpholino oligomer-induced exon skipping in *mdx* mice. *Hum Gene Ther* **20**: 955–965.
28. Yu, RZ, Baker, B, Chappell, A, Geary, RS, Cheung, E and Levin, AA (2002). Development of an ultrasensitive noncompetitive hybridization-ligation enzyme-linked immunosorbent assay for the determination of phosphorothioate oligodeoxynucleotide in plasma. *Anal Biochem* **304**: 19–25.
29. Aartsma-Rus, A, Janson, AA, Kaman, WE, Bremmer-Bout, M, den Dunnen, JT, Baas, F *et al.* (2003). Therapeutic antisense-induced exon skipping in cultured muscle cells from six different DMD patients. *Hum Mol Genet* **12**: 907–914.



This work is licensed under the Creative Commons Attribution-NonCommercial-No Derivative Works 3.0 License. To view a copy of this license, visit <http://creativecommons.org/licenses/by-nc-nd/3.0/>